



Innovative Applications of O.R.

Modeling influenza progression within a continuous-attribute heterogeneous population

Anna Teytelman, Richard C. Larson^{*}

Massachusetts Institute of Technology, Cambridge, MA 02139, USA

ARTICLE INFO

Article history:

Received 12 May 2011

Accepted 15 January 2012

Available online 25 January 2012

Keywords:

Influenza modeling

Heterogeneity

H1N1

Super-spreaders

ABSTRACT

We consider three attributes of an individual that are critical in determining the temporal dynamics of pandemic influenza: social activity, proneness to infection, and proneness to shed virus and spread infection. These attributes differ by individual, resulting in a heterogeneous population. We develop discrete-time models that depict the evolution of the disease in the presence of such population heterogeneity. For every individual, the value for each of the three describing attributes is viewed as an experimental value of a continuous random variable. The methodology is simple yet general, extending more traditional discrete compartmental models that depict population heterogeneity. Illustrative numerical examples show how individuals who have much larger-than-average values for one or more of the attributes drive the influenza wave, especially in the early generations of the pandemic. This heterogeneity-driven pandemic physics carries important policy implications. We conclude by using contact data in four European countries to demonstrate empirical uses of our model.

© 2012 Elsevier B.V. All rights reserved.

1. Introduction

Pandemic influenza is an ongoing threat to communities large and small. Despite a large body of research dealing with mathematical modeling of influenza spread, there is still no widely accepted way to inform decision making in the case of a global event such as the 2009–2010 H1N1 “swine flu” pandemic. The H1N1 influenza outbreak demonstrated that limited information and short time allowances during a pandemic make it difficult to model accurately the spread of influenza and to make appropriate and effective decisions with regard to public policy and vaccine distribution.

As a pandemic evolves, decision makers receive aggregate statistics in the form of the number of people reporting to physicians with flu-like symptoms, number of related hospital admissions, number of flu-related deaths, and number of vaccinations administered. Yet, aggregate statistics hide the fact that early transmission and propagation of the disease are driven largely by particular segments of the population: (1) those who are highly active in daily face-to-face encounters; (2) those who are overly prone to become infected given exposure; and/or (3) those who shed virus and spread the disease much more than average. Any person can be characterized along a spectrum of these three attributes: social activity, proneness to infection, and proneness to shed virus and spread infection. Those who are at the ‘right-hand-tails’ of one or

more of these distributional attributes play a significant role in the early spread of the disease. Such individuals, due to early infection, drop out of the susceptible population near the middle and almost certainly by the end of the outbreak.

The correlation between these types of heterogeneity also plays a role in the speed of infection spread aside from the usual transmissibility parameters like R_0 . It is reasonable to assume that people who are most susceptible to infection are also those that are most likely to spread it to others; the most socially active people combine these two attributes. However, a negative correlation between susceptibility and infectiousness will cause the infection to spread much slower and be sustained for a longer period of time within a community. To understand the dynamics of flu spread, or the spread of any human-to-human infectious disease, one cannot ignore such population heterogeneities.

In this paper, we generalize the heterogeneous-population, influenza-spread model of Larson [15]. We improve analytical tractability by incorporating a more general, continuous form of population heterogeneity. The generalized model allows for a more realistic heterogeneous “class” selection, which in turn increases the accuracy of the model and yet simplifies its representation.

2. Relevant modeling literature

There is an extensive literature on modeling pandemic influenza spread. The simplest and most common models for influenza spread follow some variant of the S–I–R compartmental approach

^{*} Corresponding author.

E-mail address: rclarson@mit.edu (R.C. Larson).

where each person in the population is susceptible, infected, recovered, or dead. Such models are often used in a homogeneous setting, where all people in a single compartment behave identically and there is random mixing [1,14]. This approach may be considered incomplete because it ignores population heterogeneity, the visible form of which is manifested as “super-spreaders”. The extreme cases of super-spreaders such as Typhoid Mary in the case of typhoid fever in the US [29], or Liu Janlun during the SARS outbreak [18,26], bring with them the possibility of one particularly active person sparking an outbreak even if the rest of the population is relatively weak at transmitting the infection [16,22]. More typical are the populations where some members of the population are inherently more active at spreading the disease than others. Literature on heterogeneity consistently shows that this inherent heterogeneity causes a significant impact on the dynamics of the outbreak and even whether such an outbreak occurs at all [1,15,21]. Nigmatulina and Larson showed that people who have a large number of daily contacts are the “drivers” of the infection. These people tend to get infected early in the outbreak and drive the propagation of the flu in the early stages [15,21].

Heterogeneous compartmental models are also developed in the literature. The general idea is to divide the population into a finite (usually small) number of discrete departments. People in each compartment are assumed to behave identically, with full intra-compartmental random mixing [13,23,30]. This approach involves a large number of differential equations with fixed Markovian assumptions, and needs to be solved numerically to compute the model-predicted average trends of the epidemic. In discrete-time heterogeneous models, a next-generation matrix is a useful tool in tracking an epidemic [9]. The next-generation matrix takes into account the anticipated inter-group contact rates, and uses them to calculate the number of infected individuals in each heterogeneous class of the population as the outbreak progresses. It is used in modeling early-stage epidemic growth and in estimating flu parameters, such as the *basic reproductive number*, R_0 , defined as “the expected number of secondary cases produced in a completely susceptible population by a ‘typical’ infected individual during her entire period of infectiousness” [10].

Employing an approach quite different from the traditional compartmental models, in this paper we expand on the heterogeneous modeling by Larson [15]. Larson introduced simple discrete-time modeling that took into account population heterogeneity without the need for the data that forms the next-generation matrix. Instead, he used the idea of proportional mixing, where each person is likely to get infected in proportion to his or her contact rate, as opposed to a posited specific rate of infection between each pair of classes [15,23].

In this paper we generalize Larson’s approach to eliminate the need for a finite number of discrete classes of statistically identical individuals. Instead, we introduce a continuous distribution for all the parameters in question, in essence employing an infinite number of classes. Eventually we deal with all three attributes introduced above: social activity, proneness to infection, and proneness to spread infection. Initially we focus on contact rates, the measure of social activity. The model relies on just a few equations that define the state of infection at a given time. We present numerical examples showing how various segments of the population are affected throughout the outbreak and the importance of determining a good starting distribution for contact rates. We also discuss the calculation of R_0 , and particularly the effects of heterogeneity on R_0 —the average number of secondary infections caused by a typical infectious individual at time t from the start of the outbreak. We conclude by using contact data from four European countries to demonstrate the empirical uses of our model. In addition to generalizing the traditional compartmental model by using a spectrum of heterogeneity as opposed to arbitrary classes, our

model introduces closed-form equations to describe the state of the epidemic in a community at different points in time. These equations can be used to mathematically prove results regarding the changing characteristics of the population and the progression of the virus within the community. We provide some such proofs of in Section 3.3.

3. Generalized model

Larson employs a discrete-time model where the unit of time is a generation of influenza, or a “day”. A generation for the purposes of this model is the period of infection during which a person is infectious and actively interacting in society. Larson’s model assumes a finite number of classes of people, differing by their activity level. Specifically,

λ_c = Poisson rate of human contacts per day of an individual in class C .

p = probability that a susceptible person becomes infected after a contact with an infectious individual.

During each day i , a person may be classified as susceptible, infected, or immune. A person’s state may change on day $i + 1$, where each susceptible person independently may become infected or remain susceptible, an infected person recovers and becomes immune, and each immune person remains immune. For simplicity here, we assume that there are no influenza-related deaths during this outbreak.

We generalize on this model by making the Poisson contact rate λ a random variable, and assuming a distribution of λ over the entire population. For a given person in the population, we sample from the λ -distribution and find $\lambda = \lambda_0$. Then, that person has a number of potentially infectious daily contacts n , selected from a Poisson distribution with mean λ_0 . Here λ_0 corresponds to the individual’s “class”. We introduce the following notation:

$f(\lambda)$	population distribution of λ , the individual Poisson rate of contacts per day ¹
$f_i^I(\lambda)$	distribution of λ , the individual Poisson rate of contacts per day i , in the infectious population on day. That is, if we were to select a single person, at random, from the infectious population, $f_i^I(\lambda)$ would represent the distribution corresponding to that person’s daily contact rate, λ
$f_i^S(\lambda)$	distribution of λ , the individual Poisson rate of contacts per day, in the susceptible population on day i . That is, if we were to select a single person at random from the susceptible population, $f_i^S(\lambda)$ would represent the density function corresponding to that person’s daily contact rate, λ . ²
N_t^I	number of infectious individuals on day i
N_t^S	number of susceptible individuals on day i
N	total number of people in a population

Once we know the initial conditions, we can model a typical epidemic curve and approximate the social-contact characteristics of the population by sequentially applying steps similar to those used by Larson:

¹ We assume here that $f(\lambda)$ is a continuous probability density function. The arguments in this section may also be applied to discrete distributions, for which $f(\lambda)$ represents the probability that the Poisson contact rate equals λ . We will use $f(\lambda)$ and the word “distribution” in both contexts to refer to either the probability density function or the probability mass function and use summations instead of integrals where appropriate.

² Some individuals may change their contact rates during their infectious generation, e.g. by staying at home while symptomatic. We discuss the possibility of such behavioral changes in Section 3.4.3.

Day i :

We start with the known values of all our quantities of interest during day i : $N_i^S, N_i^I, f_i^S(\lambda)$ and $f_i^I(\lambda)$.

We now show how to find all the necessary values of $N_{i+1}^S, N_{i+1}^I, f_{i+1}^S(\lambda)$ and $f_{i+1}^I(\lambda)$.

As per Larson, let

β_i = the day i probability that a random person's next interaction is with an infected person.

We now consider the total expected number of contacts that all infectious people make on day i :

$$\int_0^\infty N_i^I \lambda f_i^I(\lambda) d\lambda = N_i^I \int_0^\infty f_i^I(\lambda) d\lambda = N_i^I E_i^I(\lambda).$$

The mean total number of day i contacts by infectious people is the product of the average number of contacts by an infectious person and the number of infectious people in the population.

Likewise, the mean total number of human contacts each day is:

$$\int_0^\infty N \lambda f(\lambda) d\lambda = N \int_0^\infty \lambda f(\lambda) d\lambda = NE(\lambda).$$

and, with no behavioral changes or deaths, is assumed to be constant throughout the outbreak.

Therefore, the probability that any interaction is with an infectious person, is simply the ratio:

$$\beta_i = \frac{N_i^I E_i^I(\lambda)}{NE(\lambda)}. \quad (1)$$

We next define the day-specific infection probability:

$p_i(I|\lambda)$ = probability that a susceptible individual with contact rate λ becomes infected on day i which Larson showed to be:

$$p_i(I|\lambda) = 1 - e^{-\lambda p \beta_i}. \quad (2)$$

We now have all the necessary tools to find $N_{i+1}^S, N_{i+1}^I, f_{i+1}^S(\lambda)$ and $f_{i+1}^I(\lambda)$:

$$N_{i+1}^I = \int_0^\infty p(I|\lambda) N_i^S f_i^S(\lambda) d\lambda = N_i^S \int_0^\infty p(I|\lambda) f_i^S(\lambda) d\lambda, \quad (3)$$

$$N_{i+1}^S = N_i^S - N_{i+1}^I. \quad (4)$$

The λ -distributions over different segments of the population are slightly more complex. The distribution of contact rates of infectious people changes on day $i+1$ from what it was on day i . On day $i+1$, it is the distribution of contact rates of those people who were susceptible and became infected on day i :

$$\begin{aligned} f_{i+1}^I(\lambda) &= f(\lambda | \text{individual was infected on day } i) \\ &= \frac{p_i(I|\lambda) f_i^S(\lambda)}{\int_0^\infty p_i(I|\lambda) f_i^S(\lambda) d\lambda}. \end{aligned} \quad (5)$$

Now for the susceptibles: their day $i+1$ contact-rate distribution is that of those who were susceptible on day i and who were not infected on day $i+1$:

$$\begin{aligned} f_{i+1}^S(\lambda) &= f(\lambda | \text{individual was not infected on day } i) \\ &= \frac{(1 - p_i(I|\lambda)) f_i^S(\lambda)}{\int_0^\infty (1 - p_i(I|\lambda)) f_i^S(\lambda) d\lambda}. \end{aligned} \quad (6)$$

These formulae describe entirely the state of the epidemic in the community on day i . By starting with some known boundary values of parameters and iteratively applying these rules over time, we obtain a model of complete epidemic dynamics within a continuous heterogeneous context.

Model summary

Starting with the following quantities on day i : $N_i^S, N_i^I, f_i^S(\lambda)$ and $f_i^I(\lambda)$

Compute the intermediate quantities:

$$\beta_i = \frac{N_i^I E_i^I(\lambda)}{NE(\lambda)}$$

$$p_i(I|\lambda) = 1 - e^{-\lambda p \beta_i}$$

Compute the relevant quantities on day: $i+1$

$$N_{i+1}^I = N_i^S \int_0^\infty p_i(I|\lambda) f_i^S(\lambda) d\lambda$$

$$N_{i+1}^S = N_i^S - N_{i+1}^I$$

$$f_{i+1}^I(\lambda) = \frac{p_i(I|\lambda) f_i^S(\lambda)}{\int_0^\infty p_i(I|\lambda) f_i^S(\lambda) d\lambda}$$

$$f_{i+1}^S(\lambda) = \frac{(1 - p_i(I|\lambda)) f_i^S(\lambda)}{\int_0^\infty (1 - p_i(I|\lambda)) f_i^S(\lambda) d\lambda}$$

3.1. Numerical examples

3.1.1. Uniform distribution

We first model a population of a small hypothetical community of people. As a boundary condition, consider $f_0(\lambda)$ to be uniform between 0 and 40. Iteratively running our model, results are summarized in Figs. 1 and 2 and Table 1. Additional details are provided in Appendix C.

Talking through the example, on day 0, we introduced infectious individuals into the population, each having a λ value drawn from the uniform distribution over 0–40. However, on day 1, the distribution of contact rates of infectious persons resembles a straight line with slope $\frac{1}{8}$. That is, if on day 1 we were to select a person at random from the infectious population, that person would be much more likely to have a high daily contact rate, than a low one. In fact, the expected contact rate by an infectious person on day 1 is 26.7 (Table 1). Note, also, that it is impossible for a person from the infectious population to have a daily contact rate of 0 because a person with no contacts has no chance of being infected. The infected population becomes “high-activity” heavy. This is consistent with Larson’s model and supports the conclusion that high-activity people are the drivers of the infection at the beginning of the outbreak. As the outbreak continues, however, the high-activity tail dips down, as high-activity individuals become infected early, become immune and can no longer be infected. Note that, on the contrary, the distribution of contact rates in the susceptible population becomes more and more “low-activity” heavy. On the last day of the outbreak, the average contact rate in the susceptible population is 10.4, almost half of the original average contact rate of 20.

3.1.2. Poisson distribution

We now consider the same community with different initial conditions. We propose a more realistic, Poisson distribution for $f(\lambda)$ with mean 20. Firstly, we are now dealing with a discrete distribution for λ as opposed to a continuous density function. Fig. 3 describes the progression of the outbreak with some notable differences from the first example.

Here too, we see that the characteristics of the subsections of the population change as the outbreak continues, although the effect is much smaller. On the first day, the expected contact rate in the infectious population is 21, a slight increase from 20 (Table 2).

Toward the end, the expected contact rates in different subsections of the population change slightly, but generally the distributions remain similar to the original contact rate distribution,

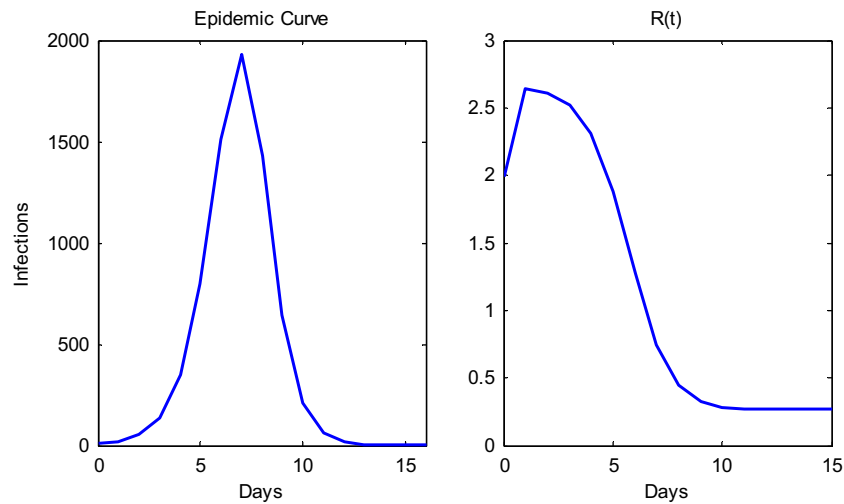


Fig. 1. Under an initial uniform distribution of daily contact rates, the epidemic curve and $R(t)$ of the outbreak. $R(t)$ is computed by dividing the number of infectious people at time $t + 1$ by the number of infectious people at time t .

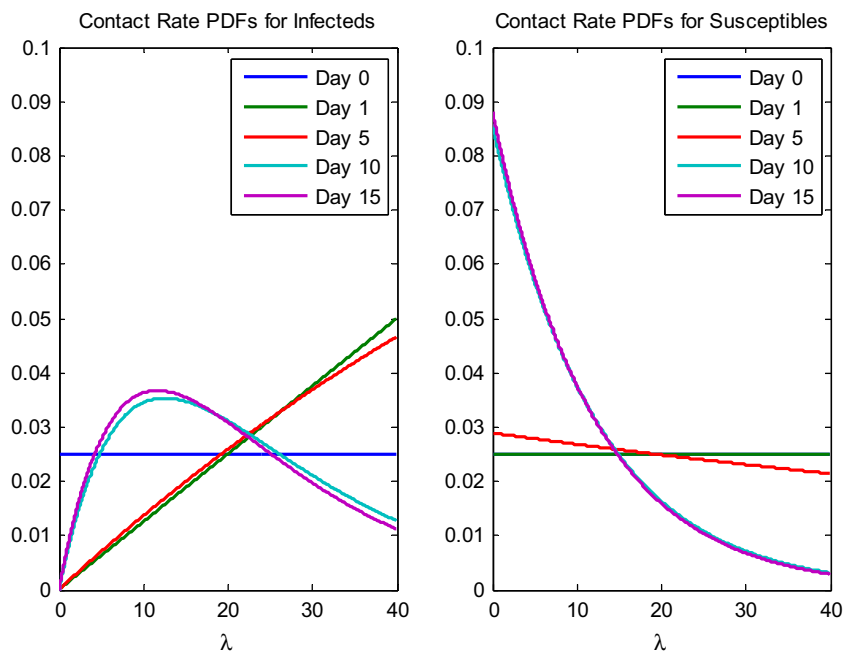


Fig. 2. Contact rate characteristics for the infectious and susceptible subsections of the population at different times during the outbreak.

Table 1

Outbreak statistics. The initial distribution of λ is uniform between 0 and 40.

Outbreak statistics	
Duration of outbreak	17 days
Total number of infections	7168
$E_1^I(\lambda)$	26.7
$E_{17}^I(\lambda)$	18.2
$E_{17}^S(\lambda)$	10.4

(Fig. 4). This behavior is noticeably different from the changing distributions in the uniform distribution case.

3.2. Sensitivity to original distribution

The two numerical examples show that the original distribution of contact rates plays a major role in the evolution of all four of our

relevant quantities. The total expected number of infections in the outbreak is 10% larger in the case of a Poisson original distribution than in the case of a uniform distribution. In the case of the uniform distribution, the susceptible and the infectious subsections of the populations have extremely different contact rate characteristics. The susceptible population is low-activity heavy, while the contact rate distribution for the infectious population is a concave function with low probability at the left tail and decreasing probability at the right.

3.2.1. Calculation of R_0

The differences between the two cases are particularly evident in the calculation of the basic reproductive number, R_0 . Recall that R_0 is defined as the expected number of secondary infections caused by a typical infected individual in a fully susceptible population [10]. On day 0, since almost everybody is susceptible, we can assume that we are in a fully susceptible population. There is some

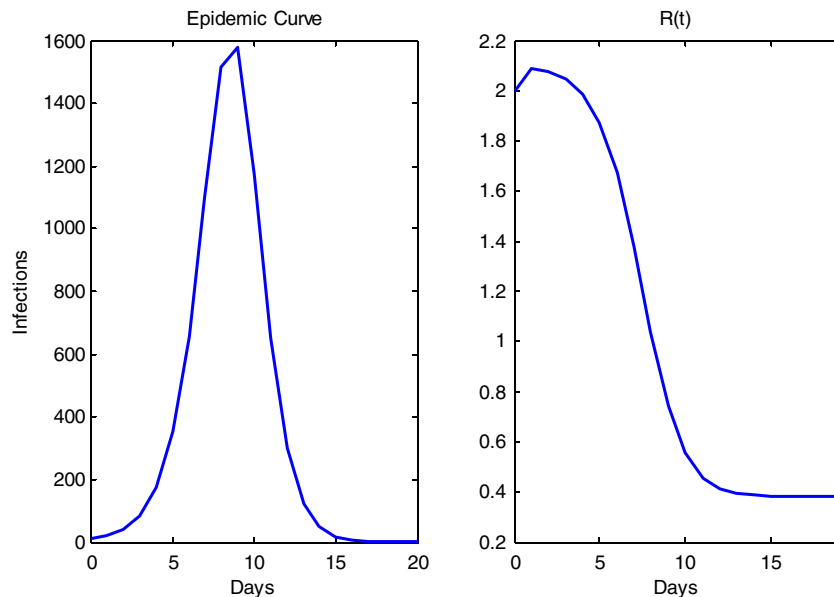


Fig. 3. The epidemic curve and $R(t)$ of the outbreak. The initial distribution is Poisson with mean 20.

Table 2
Outbreak statistics. The initial distribution of λ is Poisson with mean 20.

Outbreak statistics	
Duration of outbreak	21 days
Total number of infections	7865
$E_1^I(\lambda)$	21.0
$E_{20}^I(\lambda)$	19.5
$E_{\infty}^S(\lambda)$	18.4

uncertainty as to the exact manner of calculating R_0 . The cause of ambiguity is the term “typical”. Suppose we pick a person at random from our infectious population on day 0. In both the case of the uniform and the Poisson original distributions, the average contact rate for a random person, call her patient zero, would be

20. If the Poisson contact rate is 20, the average number of patient zero’s contacts is also 20. Since each contact has .1 probability of spreading infection, this interpretation of the definition would give us an R_0 of 2. If R_0 is the same for both original distributions of contact rates, we would expect the total number of infections to be approximately the same, but they are not.

Instead, we recommend the logic followed by network models in the established epidemiological literature [9,10,19], where R_0 is calculated as an expected value of a distribution that is weighted by the magnitude of the contact rate. That is, a person in the infectious population with a high contact rate should be weighed proportionally higher, as that person is more likely to acquire and then spread the infection than a person with a low contact rate. In other words, our “typical” person would no longer be selected at random, but according to a distribution $f_R(\lambda)$. Such a distribution will no longer be sampling from the population of people, but rather

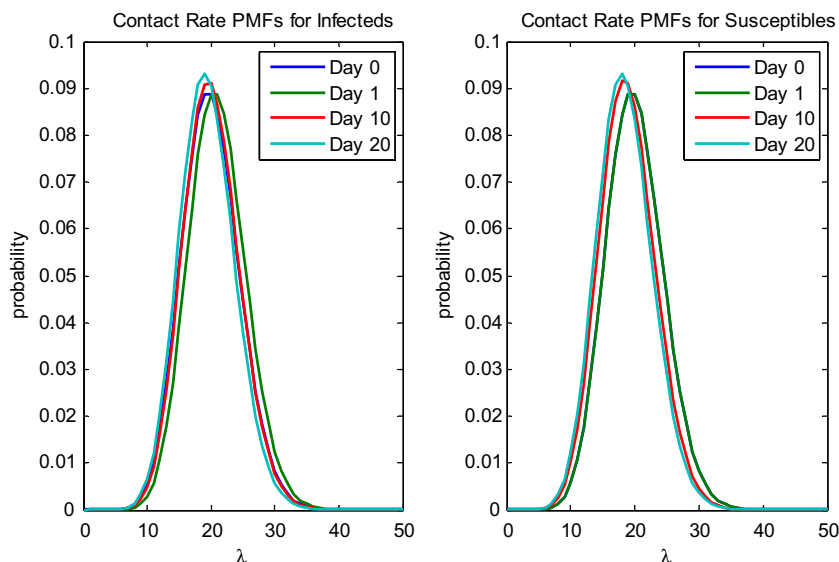


Fig. 4. Contact rate characteristics for the infectious and susceptible subsections of the population at different times during the outbreak. The initial distribution is Poisson with mean 20.

population of contacts. Consider each person dropping a piece of paper that is marked with that person's λ value on the floor during each and every contact. We then pick R_0 by drawing a random piece of paper. This new distribution would favor high activity people proportionally to their activity level, then $f_R(\lambda) = \frac{f_0^i \lambda}{E_0^i(\lambda)}$.

Note that this is exactly the formula used to describe the concept of time-average duration of an interval in a renewal process [12]. Using this scenario, we can calculate R_0 . For the uniform distribution case:

$$R_0 = \int_0^{40} p \frac{\lambda^2}{40E(\lambda)} d\lambda \frac{40^2}{30 * 20} = 2.7.$$

For the Poisson case:

$$R_0 = \sum_0^\infty p \frac{\lambda^2}{E(\lambda)\lambda!} e^{-20} = \frac{420}{200} = 2.1.$$

Note that even though the uniform distribution has a larger value of R_0 , it actually results in fewer total infections! This phenomenon is caused by the fact that the uniform distribution has a higher variance than a Poisson distribution with the same mean. In the uniform case, there are fewer very high-activity people who are depleted much more quickly than in the Poisson case. Once the high-activity people are gone, the outbreak quickly subsides resulting in a shorter total outbreak time and fewer total infections. It is important to note, also, that the effect of depletion of high-activity individuals from the population comes from the fact that high-activity people are more susceptible to infection; we show in Section 3.4.2, that the fact that these people are also more infectious does not contribute to this effect. Andersson and Britton [2] confirm, using compartmental model methods, that epidemics are particularly devastating when susceptibility does not vary, i.e. there is no early depletion.

This is another reminder that an influenza model is a simplification of a real life problem that is too complex to describe fully. To avoid critical mistakes, healthcare decision-makers must be extremely cautious in choosing initial values of the model's parameters such as the initial distribution of contact rates to avoid critical mistakes. Many published heterogeneous modeling published papers describe deriving R_0 in a manner consistent with the second approach above, arguing that R_0 is the mean of a distribution that is skewed toward high-activity individuals [9,10,19]. However, one needs to be careful when transferring this idea into simulation modeling. Often, we find that flu simulations are seeded by selecting a few typical "patient zeros" from the population to enter the susceptible population in an infectious state. These typical people are selected to be representative of the overall general population, and their average contact rate is used to calibrate the simulation to known R_0 parameters. "Patient zeros" that are selected in this way, result in an underestimate of the true value of R_0 .

3.3. Common properties

Despite the fact that the starting distribution plays a significant role in the way an epidemic curve for the outbreak is calculated using this model, certain properties remain true regardless of original distribution.

Theorem 1 (Tilting of contact rate distributions in susceptible and infected populations). Starting with any initial conditions, $f_0^i(\lambda)$ and $f_0^s(\lambda)$: for any $(i > 0)$:

$$f_0^i(\lambda) = C_i^l \left(e^{-\lambda p \sum_{j=0}^{i-1} \beta_j} - e^{-\lambda p \sum_{j=0}^i \beta_j} \right) f_0^s(\lambda), \quad (7)$$

and

$$f_i^s(\lambda) = C_i^s \left(e^{-\lambda p \sum_{j=0}^{i-1} \beta_j} \right) f_0^s(\lambda), \quad (8)$$

where C_i^l and C_i^s are normalizing constants. Equations (7) and (8) imply that as the outbreak progresses, contact rate distributions become tilted distributions with tails decaying exponentially faster than in the original contact rate distributions. Note also, that the initial distribution of infectious individuals, $f_0^i(\lambda)$, plays no role in the distributions for any generation $i > 0$.

Proof. ³

We next introduce a result that will be useful in describing the behavior of distributions as the outbreak progresses in more detail.

Lemma 1. For any constants $0 < a \leq 1$, $0 < b \leq 1$, and $\lambda > 0$ the function:

$$g(\lambda) = \left(\frac{(1 - e^{-\lambda a})}{(e^{\lambda b} - 1)} \right)$$

is monotonically decreasing and convex in λ .

Theorem 2. Stochastic ordering of susceptible and infectious populations. Let A_i^s be the random variable distributed as $f_i^s(\lambda)$, and similarly A_i^i as $f_i^i(\lambda)$. Then, as long as $f_0^s(\lambda), f_0^i(\lambda)$ are non-deterministic, for any $i > 0$:

$$A_{i+1}^s <_{ST} A_i^s \quad \text{for } \lambda \geq E_i^s(\lambda), \quad (9)$$

$$A_i^s <_{ST} A_i^i \quad \text{for } \lambda \geq E_i^s(\lambda), \quad (10)$$

$$A_{i+1}^i <_{ST} A_i^i \quad \text{for } \lambda \geq E_i^s(\lambda), \quad (11)$$

where $X <_{ST} Y$ implies that X is strictly smaller than Y in the usual stochastic order [24]. Stochastic ordering of the various distributions as time goes on provides us with an analytical expression of our intuition. That is, according to Eq. (9), the contact rates in the susceptible population become "smaller" with time in the stochastic ordering sense. In other words, the susceptible population becomes more and more densely packed with inactive individuals as the high activity people become infected. Similarly with the infectious population.

Theorem 3. Depletion of high-activity individuals in the susceptible and infectious populations. As long as $f_0^s(\lambda), f_0^i(\lambda)$ are non-deterministic, for any $i > 0$:

$$f_i^s > f_{i+1}^s \quad \text{for } \lambda \geq E_i^s(\lambda), \quad (12)$$

$$f_i^s <_{ST} f_{i+1}^i \quad \text{for } \lambda \geq E_i^s(\lambda), \quad (13)$$

$$f_i^i >_{ST} f_{i+1}^i \quad \text{for } \lambda \geq E_i^s(\lambda). \quad (14)$$

These are true regardless of initial contact rate distribution. Eq. (12) implies that after the first generation, the susceptible population becomes increasingly low-activity heavy. In Eq. (14) we show that the distribution of infected people also becomes more low-activity heavy with time since high-activity people become depleted from the population. For illustration, see Fig. 5. We note that since we model infection spread in discrete time increments, the high-activity people get infected in large numbers within each generation. However, in a real-life scenario, these generations overlap and we do not need to "wait for a generation to end" for new people to get infected. As a result, the depletion of high activity individuals should occur even more rapidly in a continuous-time, real-world outbreak. Finally, we note that expectation

³ All proofs in this section are presented in Appendix A.

Lemma 3 Illustration

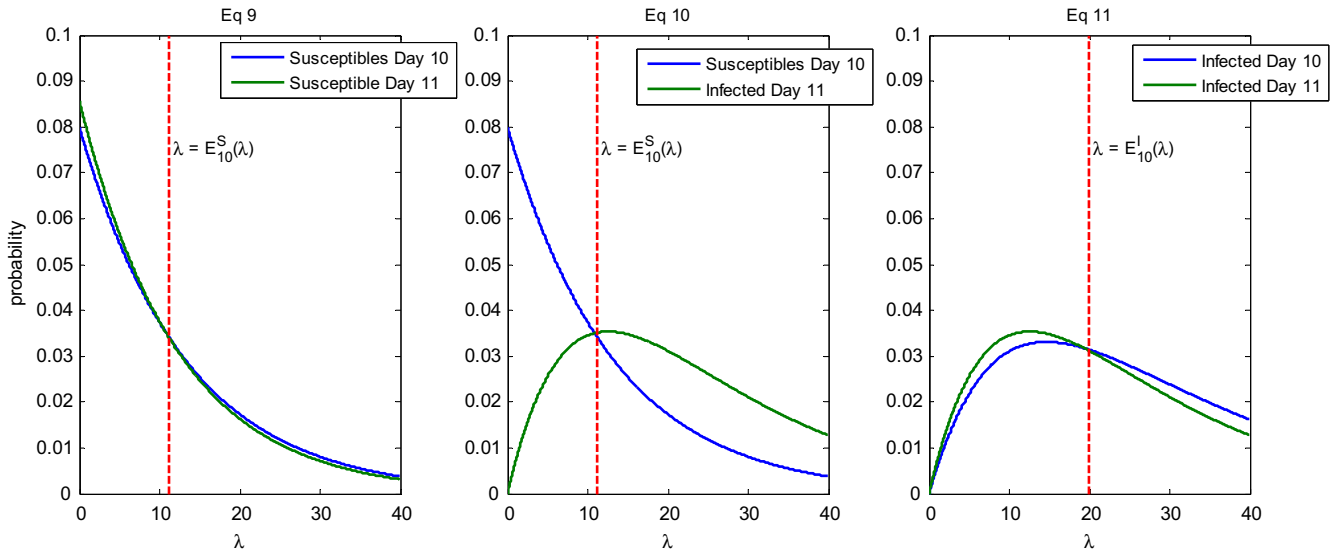


Fig. 5. Illustration to [Theorem 3](#): the probability density functions of contact rates for the susceptible and infected populations on days 10 and 11. The initial distribution of contact rates was uniform, ranging from 0 to 40.

of contact rate distributions in both the susceptible and infected subsections of the population is decreasing with time.

Corollary 1. Overall decrease in expected contact rates. For $i > 0$ and non-deterministic $f_0^S(\lambda), f_0^I(\lambda)$:

$$E_i^S(\lambda) < E_{i+1}^S(\lambda), \quad (15)$$

$$E_i^I(\lambda) < E_{i+1}^I(\lambda). \quad (16)$$

3.4. Further generalizations

The methodology developed above can be extended to include heterogeneity due to vulnerabilities of different groups as well as the effects of changing social behaviors during an ongoing pandemic.

3.4.1. Mortality

So far in our model, we have assumed that all infected people recover and rejoin the population within one generation. However, any devastating pandemic influenza that we fear is likely to be deadly; some infected individuals are likely to die of the infection. Moreover, the likelihood of death from an infection will almost certainly not be uniform throughout the population. The Centers for Disease Control and Prevention (CDC) suggests that pregnant women and the elderly are at most risk from death during a seasonal influenza outbreak [6,17]. Meanwhile, one of the characteristics of a particularly dangerous novel influenza strain pandemic, is the heightened mortality rates of the people in their 20s [27].

To add this layer of complexity, we add a probability of death after an infection, q . That is, an infectious person dies at the end of her infectious period with probability q , and rejoins the population with probability $(1 - q)$. Moreover, this probability cannot be constant, as certain people are at more risk than others. We must impose a probability distribution on q that is not independent from λ .

The quantities of interest become:

$f(\lambda, q)$ the joint distribution of λ , the Poisson rate of contacts per day and, q the probability of death given infection, in the entire population alive at the start of day i

$f_i^I(\lambda, q)$ the joint distribution of λ , the Poisson rate of contacts per day, and q , the probability of death given infection, in the infectious population on day i

$f_i^S(\lambda, q)$ the joint distribution of λ , the Poisson rate of contacts per day, and q , the probability of death given infection, in the susceptible population on day i

N_i the number of people alive in the population at the start of day i

N_i^I, N_i^S as before

Replicating Eqs. (1)–(6):

The total number of contacts made by infectious people on day i remains as before:

$$\int_0^1 \int_0^\infty N_i^I \lambda f_i^I(\lambda, q) d\lambda dq = N_i^I \int_0^1 \int_0^\infty \lambda f_i^I(\lambda, q) d\lambda dq = N_i^I E_i^I(\lambda).$$

However, the total number of interactions made by the entire population on day i , now needs to account for the mortality rate of the population:

$$\int_0^1 \int_0^\infty N_i \lambda f_i(\lambda, q) d\lambda dq = N_i \int_0^1 \int_0^\infty \lambda f_i(\lambda, q) d\lambda dq = N_i E_i(\lambda).$$

We can now solve for β_i :

$$\beta_i = \frac{N_i^I E_i^I(\lambda)}{N_i E_i(\lambda)}. \quad (1a)$$

The dynamics of the spread of infection on day i remain unchanged as the deaths occur at the end of each generation; Eqs. (3)–(6) remain unchanged except for the new distribution functions that account for death probabilities.

$$N_{i+1}^I \int_0^1 \int_0^\infty p(I|\lambda) N_i^S f_i^S(\lambda, q) d\lambda dq = N_i^S \int_0^1 \int_0^\infty p(I|\lambda) f_i^S(\lambda, q) d\lambda dq, \quad (3a)$$

$$N_{i+1}^I = N_i^S - N_{i+1}^I, \quad (4a)$$

$$f_{i+1}^I(\lambda, q) = \frac{p(I|\lambda) f_i^S(\lambda, q)}{\int_0^\infty p(I|\lambda) f_i^S(\lambda, q) d\lambda}, \quad (5a)$$

$$f_{i+1}^l(\lambda, q) = \frac{(1 - p(I|\lambda))f_i^s(\lambda, q)}{\int_0^\infty (1 - p_i(I|\lambda))f_i^s(\lambda, q)d\lambda}. \quad (6a)$$

We are left to find the effects of the deaths on day i . Consider the probability that a person with contact rate λ and mortality probability q died in period i :

$$P_i(\text{death}|\lambda, q) = P_i(\text{infection}|\lambda, q)q, \\ P_i(\text{infection}|\lambda, q) = \frac{f_i^l(\lambda, q) \frac{N_i^l}{N_i}}{f_i(\lambda, q)} = \frac{f_i^l(\lambda, q) N_i^l}{f_i(\lambda, q) N_i},$$

for all values of λ, q for which $f_i(\lambda, q) > 0$.

So the probability that a person with these parameters survived day i , is then:

$$1 - \frac{f_i^l(\lambda, q) N_i^l}{f_i(\lambda, q) N_i} q.$$

We can then derive $f_{i+1}(\lambda, q)$:

$$f_{i+1}(\lambda, q) = \frac{f_i(\lambda, q) P_i(\text{no death}|\lambda, q)}{P(\text{no death})} = \frac{f_i(\lambda, q) \left(1 - \frac{f_i^l(\lambda, q) N_i^l}{f_i(\lambda, q) N_i} q\right)}{1 - \frac{N_i^l E_i(q)}{N_i}}, \quad (17)$$

and finally, assuming that deaths are independent of each other:

$$N_{i+1} = N_i - N_i^l \int_0^1 \int_0^\infty q f_i^l(\lambda, q) d\lambda dq = N_i - N_i^l E_i(q). \quad (18)$$

3.4.2. Variability in susceptibility and infectivity

The second additional layer of complexity is also acknowledged by Larson. We have so far assumed that if a susceptible and infectious individual come into contact, regardless of their respective contact rates, the probability that a susceptible person becomes infected from the contact is p . However, particularly in recent times, there has been added concern about people who are inherently more susceptible to disease than others. For example, the recent H1N1 pandemic of 2009 was shown to be less likely to affect people over 65 [5]. The “Asian Flu” of 1957 reported similar tendencies most likely due to acquired immunity by the older generation. Similarly, some portion of the population includes “super-shedders”; these people are much more likely to spread the disease than the average person. These differences in people’s ability to shed and be infected by the flu virus, cause variability in the parameter p .

Larson brings up this possibility by splitting p into two different parameters. We will change notation here to call these parameters r and s .

r = the infectiousness index of an individual. r can take on any value between 0 and 1; it describes the level of infectiousness of an individual, with 0 implying a person does not shed any virus, and 1 implying a person is maximally infectious.

s = the level of susceptibility of an individual. That is, the probability that a susceptible individual gets infected after an interaction with an infectious individual with infectiousness index $r = 1$.

Using this notation, if an infectious person with infectiousness index r and a susceptible person with susceptibility parameter s make contact on a given day, the probability that the susceptible person becomes infected is $p = r * s$

We alter our epidemic parameters to include r and s :

$f_i(\lambda, q, r, s)$ = joint distribution of λ, q, r , and s in the entire population alive at the start of day i .

$f_i^l(\lambda, q, r, s)$ = joint distribution of λ, q, r , and s in the infectious population on day i .

$f_i^s(\lambda, q, r, s)$ = joint distribution of λ, q, r , and s in the susceptible population on day i .

N_i = number of people alive in the population at the start of day i .

N_i^l, N_i^s as before.

Once again we calculate equations analogous to Eqs. (1)–(6), taking extra care with notation:

$\beta_i(r)$ = the probability that a random person’s next interaction is with an infected person having infectivity parameter r , on day i .

$$\beta_i(r) = \frac{\int_0^1 \int_0^1 \int_0^\infty N_i^l \lambda f_i^l(\lambda, q, r, s) d\lambda dq ds}{\int_0^1 \int_0^1 \int_0^\infty N_i \lambda f_i(\lambda, q, r, s) d\lambda dq dr ds} = \frac{N_i^l E_i^l(r) f_i^l(r)}{N E(\lambda)}. \quad (1b)$$

Let:

$p_i(I|\lambda, q, s)$ = Probability that a susceptible person with susceptibility parameter s and contact-rate parameter λ , becomes infected on day i (note that the person’s value of r is irrelevant), (2b)

$$p(I|\lambda, q, s) = 1 - e^{-\lambda s \int_0^2 \hat{r} \beta_i(\hat{r}) d\hat{r}}.$$

See Larson [15] supplementary materials for derivation.

Then we calculate the usual quantities:

$$N_{i+1}^l = N_i^l \int_0^1 \int_0^1 \int_0^\infty p(I|\lambda, q, s) f_i^s(\lambda, q, r, s) d\lambda dq dr ds, \quad (3b)$$

$$N_{i+1}^l = N_i^s - N_{i+1}^l, \quad (4b)$$

$$f_{i+1}^l(\lambda, q, r, s) = \frac{p_i(I|\lambda, q, s) f_i^s(\lambda, q, r, s)}{\int_0^1 \int_0^1 \int_0^\infty p(I|\lambda, q, s) f_i^s(\lambda, q, r, s) d\lambda dq dr ds}, \quad (5b)$$

$$f_{i+1}^s(\lambda, q, r, s) = \frac{(1 - p_i(I|\lambda, q, s)) f_i^s(\lambda, q, r, s)}{\int_0^1 \int_0^1 \int_0^\infty (1 - p(I|\lambda, q, s)) f_i^s(\lambda, q, r, s) d\lambda dq dr ds}, \quad (6b)$$

$$f_{i+1}(\lambda, q, r, s) = \frac{f_i(\lambda, q, s) \left(1 - \frac{f_i^l(\lambda, q, r, s) N_i^l}{f_i(\lambda, q, r, s) N_i}\right)}{1 - \frac{N_i^l E_i(q)}{N_i}}, \quad (14b)$$

and

$$N_{i+1} = N_i - N_i^l E_i(q). \quad (15b)$$

3.4.3. Behavioral changes

We have so far been working with a static model, where people behave in the same way every day and do not change their routine as influenza enters their community. However, previous outbreaks such as the 2002 SARS epidemic show evidence that people change their behavior throughout their outbreak even if their region has not yet been affected by the epidemic [21,25]. These behavioral changes have been shown to make an impact on the spread of infection. A good model, therefore, should take into account the fact that people will try to limit their daily activity in the event of a pandemic scare [21].

This can be easily incorporated our model by introducing a transformation function $G_i(\lambda)$ that represents the effect of behavioral changes in λ on day i . If G is invertible, the distribution functions can be easily determined at the end of each day.

On day i consider the quantities $f_i^*(\lambda, q, r, s), f_i^l(\lambda, q, r, s)$ and $f_i^s(\lambda, q, r, s)$ to be the relevant distributions computed without taking into account behavioral interventions. Then:

$$f_i(\lambda, q, r, s) = f_i^*(G_i(\lambda), q, r, s),$$

$$f_i^l(\lambda, q, r, s) = f_i^{l*}(G_i(\lambda), q, r, s),$$

$$f_i^s(\lambda, q, r, s) = f_i^{s*}(G_i(\lambda), q, r, s).$$

For example, we can assume that each day, all individuals reduce their number of contacts by a factor of $\frac{1}{10}$. Then $G_i(\lambda) = \frac{9}{10}\lambda$, and the distributions are changed accordingly. This is a simple example of how the model can be used to reflect dynamic behavioral changes during the outbreak. The model can be extended further and made arbitrary complex by using non-deterministic or state-based functions for partial compliance with government programs.

3.5. European data

We conclude with an example based on research by Mossong et al. In this section, we will use the word ‘day’ to refer to an actual real-time day, and the word ‘generation’ to refer to a generation of influenza. The Mossong group conducted a thorough study of contacts by participants in eight European countries. Participants were asked to record their daily contacts, “defined as either skin-to-skin contact such as a kiss or handshake... or a two-way conversation with three or more words in the physical presence of another person” [20]. The information from the participants’ diaries was weighed to match the demographics of participating countries. The group published distributions of daily contacts by individuals from each country. We ran our model on the populations of four of those countries, namely, Belgium, Great Britain, Germany, and Poland, to demonstrate empirical use of our model.

To incorporate this information into our model, we note that these data were selected by sampling distinct persons and noting the number of contacts that person had in one day. This is not exactly $f(\lambda)$ as we have defined it for two reasons. Firstly, $f(\lambda)$ is the distribution of contact rates within a generation, not one day. To correct for this, we assumed that a generation of the flu is approximately 2.5 days [31,28], and extrapolated the available data accordingly. Secondly, $f(\lambda)$ is the distribution of *contact rates* within a population, and not the distribution of the number of *daily contacts by an individual*, which is the quantity being sampled. Recall that the number of daily contacts by a person is Poisson distributed with mean λ . Each sample point in the empirical data is a value picked from this Poisson distribution. However, we note that this empirical distribution is the maximum-likelihood estimator for $f(\lambda)$ in a specific country and we used it to estimate $f(\lambda)$ for our model. If the data from Mossong constitute a representative sample of the population, then the daily contact distribution should be equivalent to $f(\lambda)$. We used the same basic parameters for each country, so that the only differences between countries affecting the epidemic curve were their respective sizes and their contact rate distributions. Finally, note that in this example we model

heterogeneity based solely on contact rates, and none of the other possible heterogeneous parameters (see Tables 3 and 4).

Table 5 summarizes the results of our model for each of the four countries. Figs. 6 and 7 further illustrate the epidemic curves and the characteristics of the population before and after the outbreaks.

It is not surprising with all transmissibility parameters being equal, that the R_0 as well as the total number of infections caused by the outbreak is correlated with the mean contact rate in the population. It is also worth noting, that as suggested in our model analysis, the variance in the contact rates in the country is correlated with change in the susceptible population characteristics that occurred throughout the outbreak, see Table 6. Recall, also, that variance plays a role in the R_0 calculations, and as a result while Belgium and Great Britain have similar average contact rates in their respective populations, the values of R_0 for the two countries differ.

Higher variance implies that a country has a combination of highly active people and relatively non-active people in its population. During the first few generations of the outbreak, the high activity super-spreaders become infected and immune, while the susceptible population becomes dominated by low-activity individuals.

4. Discussion

Current policy literature gives little consideration to changing characteristics of the population seen throughout the outbreak. However, an argument can be made, that heterogeneity should play a significant role in certain policy decisions. Consider for

Table 5

The results of running the model using initial parameters described in Tables 3 and 4.

	Belgium	Great Britain	Germany	Poland
<i>Results</i>				
R_0	1.98	1.66	1.33	2.54
Total	4,620,000	25,780,000	15,788,000	23,787,000
infections	(44%)	(41%)	(19%)	(62%)
Duration	103 days	118 days	258 days	83 days

Table 3
Initial global parameters used in model instance.

Basic parameters	
$q(\lambda)$.002 (estimated H1N1 mortality rate) [7]
p	.04
N_i	10

Table 4
Initial country dependent parameters used in model.

	Belgium	Great Britain	Germany	Poland
<i>Country-dependent parameters</i>				
Population	10,423,493	62,348,447	82,282,988	38,463,689
	[8]	[8]	[8]	[8]
Average daily contact rate	11.84	11.74	7.95	16.31

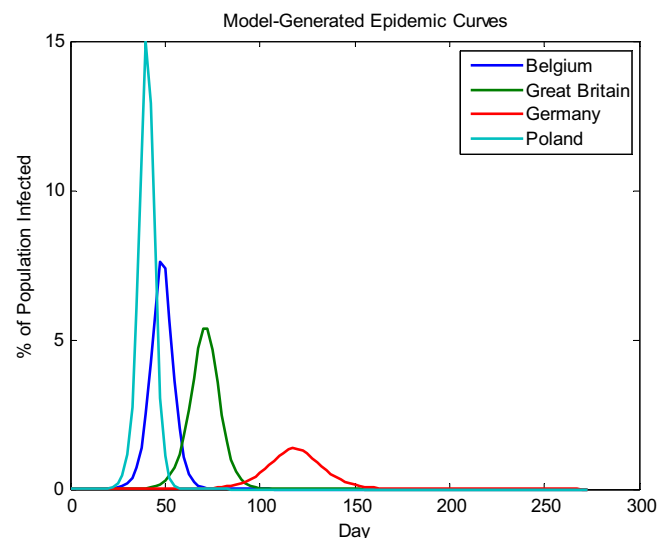


Fig. 6. Epidemic curves for the 4 countries as percentage of the population infected on a given day.

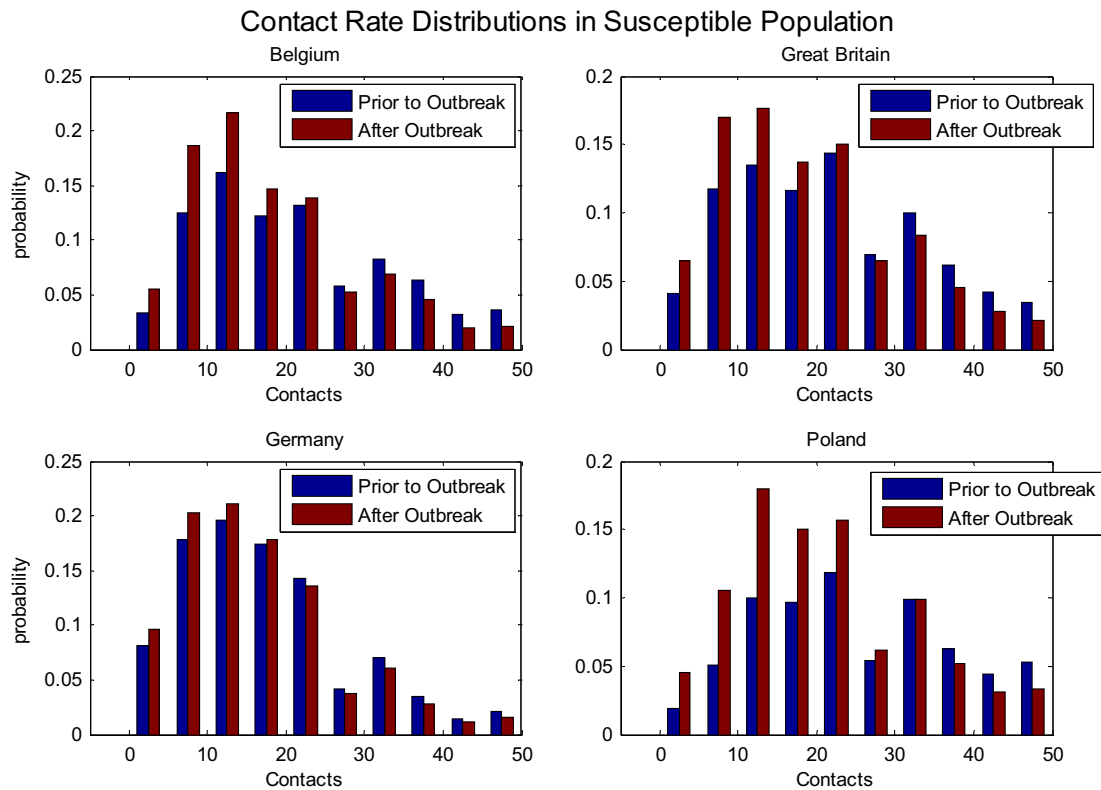


Fig. 7. The contact rate distributions in the susceptible population of each country before the beginning and after the end of the outbreak.

Table 6

The variance of a region's contact rate distribution compared to the total change in its population characteristics.

	Belgium	Great Britain	Germany	Poland
<i>Contact rate variance and population characteristic change</i>				
Contact rate variance	9.85	7.67	6.26	11.45
Mean square population change	6.6e−005	4.8e−005	1.0e−005	6.6e−004

example, vaccine administration. In a population with little heterogeneity and low contact rate variance, the characteristics do not change significantly throughout the outbreak, and vaccines administered early in an outbreak reach similar classes of people as vaccines administered later on. In a high-variance population, vaccines administered early will be more likely given to high-activity people, whereas vaccines administered later on will be particularly ineffective, as most of the recipients will already be low-activity individuals. We must not forget, however, that other considerations must play a role in policy decisions. Researchers have suggested that it is often preferable to vaccinate high-risk individuals like pregnant women and people with comorbidities [17]. However, mathematical models such as this one may provide insights into when and why activity-focused vaccination policies may be preferable.

The model we provide in this paper is generalizes existing heterogeneous compartmental models. The continuous spectrum of heterogeneous properties allows modelers a natural alternative to discrete compartments with identical individuals and proportional inter-compartmental mixing. Inclusion of heterogeneity in population modeling is especially important in policy decisions such as occur in designing vaccine allocation plans and message-

targeting in public awareness campaigns. The framework we provide not only simplifies modeling heterogeneous populations, but also provides insight into changes of population attributes over time. The closed form equations describing evolving population characteristics should invite further mathematical analysis of epidemics.

Acknowledgements

Work on this manuscript was supported by the Sloan Foundation of New York under a grant entitled, "Decision-Oriented Analysis of Pandemic Flu Preparedness & Response", and under a cooperative agreement with the US Centers for Disease Control and Prevention (CDC), Grant No. 1 P01 TP000307-01, "Linking Assessment and Measurement to Performance in PHEP Systems (LAMPS)", awarded to the Harvard School of Public Health Center for Public Health Preparedness (HSPHCPHP) and the Massachusetts Institute of Technology (MIT), Center for Engineering Systems Fundamentals (CESF). The discussion and conclusions in this paper are those of the authors and do not necessarily represent the views of the Sloan Foundation, the CDC, the US Department of Health and Human Services, Harvard or MIT. For helpful discussions on earlier drafts we thank Dr. Stan Finkelstein, Dr. Sahar Hashmi, Julia Hopkins and Kallie Hedberg. We also thank two anonymous referees for suggestions that improved the paper.

Appendix A. Proofs

Theorem 1. Starting with any initial conditions, $f_0^i(\lambda)$ and $f_S^i(\lambda)$; for any $i > 0$:

$$f_i^I(\lambda) = C_i^I \left(e^{-\lambda p \sum_{j=0}^{i-2} \beta_j} - e^{-\lambda p \sum_{j=0}^{i-1} \beta_j} \right) f_0^S(\lambda), \quad (\text{A.7})$$

$$f_i^S(\lambda) = C_i^S \left(e^{-\lambda p \sum_{j=0}^{i-1} \beta_j} \right) f_0^S(\lambda), \quad (\text{A.8})$$

Where C_i^I and C_i^S are normalizing constants.

Proof. We proceed by induction. Suppose that for some $i > 0$,

$$f_i^I(\lambda) = C_i^I \left(e^{-\lambda p \sum_{j=0}^{i-2} \beta_j} - e^{-\lambda p \sum_{j=0}^{i-1} \beta_j} \right) f_0^S(\lambda),$$

$$f_i^S(\lambda) = C_i^S \left(e^{-\lambda p \sum_{j=0}^{i-1} \beta_j} \right) f_0^S(\lambda),$$

Then

$$\begin{aligned} f_{i+1}^I(\lambda) &= \frac{p_i(I|\lambda) f_i^S(\lambda)}{\int_0^\infty p_i(I|\lambda) f_i^S(\lambda) d\lambda} = C_{i+1}^I (1 - e^{-\lambda p \beta_i}) \left(e^{-\lambda p \sum_{j=0}^{i-1} \beta_j} \right) f_0^S(\lambda) \\ &= C_{i+1}^I \left(e^{-\lambda p \sum_{j=0}^{i-1} \beta_j} - e^{-\lambda p \sum_{j=0}^i \beta_j} \right) f_0^S(\lambda). \end{aligned}$$

Since is a constant $\int_0^\infty p_i(I|\lambda) f_i^S(\lambda) d\lambda$. Similarly:

$$\begin{aligned} f_{i+1}^S(\lambda) &= \frac{(1 - p_i(I|\lambda)) f_i^S(\lambda)}{\int_0^\infty (1 - p_i(I|\lambda)) f_i^S(\lambda) d\lambda} = C_{i+1}^S (e^{-\lambda p \beta_i}) \left(e^{-\lambda p \sum_{j=0}^{i-1} \beta_j} \right) f_0^S(\lambda) \\ &= C_{i+1}^S \left(e^{-\lambda p \sum_{j=0}^i \beta_j} \right) f_0^S(\lambda). \end{aligned}$$

Now for the base case; note that since there were no infected people prior to day 0, $\beta_{-1} = 0$:

$$\begin{aligned} f_1^I(\lambda) &= \frac{p_0(I|\lambda) f_0^S(\lambda)}{\int_0^\infty p_0(I|\lambda) f_0^S(\lambda) d\lambda} = C_1^I (1 - e^{-\lambda p \beta_0}) f_0^S(\lambda) \\ &= C_1^I (1 - e^{-\lambda p \beta_0}) (e^{-\lambda p \beta_{-1}}) f_0^S(\lambda) \\ &= C_1^I \left(e^{-\lambda p \sum_{j=0}^{-1} \beta_j} - e^{-\lambda p \sum_{j=0}^0 \beta_j} \right) f_0^S(\lambda), \end{aligned}$$

and

$$\begin{aligned} f_1^S(\lambda) &= \frac{(1 - p_0(I|\lambda)) f_0^S(\lambda)}{\int_0^\infty (1 - p_0(I|\lambda)) f_0^S(\lambda) d\lambda} = C_1^S e^{-\lambda p \beta_0} f_0^S(\lambda) = C_1^S (e^{-\lambda p \beta_0}) \\ &= C_1^S \left(e^{-\lambda p \sum_{j=0}^0 \beta_j} \right) f_0^S(\lambda) \quad \square \end{aligned}$$

Lemma 1. For any constants $0 < a \leq 1$, $0 < b \leq 1$, the function:

$$g(\lambda) = \left(\frac{(1 - e^{-\lambda a})}{(e^{\lambda b} - 1)} \right)$$

is monotonically decreasing and convex in λ for $\lambda > 0$.

Proof. We first prove convexity.

Let $\lambda b = \alpha$ and $\frac{a}{b} = \gamma$ and $h(\alpha) = \left(\frac{(1 - e^{-\alpha \gamma})}{(e^\alpha - 1)} \right)$. Then $g(\lambda)$ is convex in λ if and only if $h(\alpha)$ is convex in α . Differentiating:

$$\frac{d^2 h}{d\alpha^2} = \frac{e^{-\alpha \gamma} ((e^{2\alpha} + e^\alpha) e^{\alpha \gamma} + (-e^{2\alpha} + 2e^\alpha - 1) \gamma^2 + (2e^\alpha - 2e^{2\alpha}) \gamma - e^{2\alpha} - e^\alpha)}{e^{3\alpha} - 3e^{2\alpha} + 3e^\alpha - 1}.$$

The denominator $e^{3\alpha} - 3e^{2\alpha} + 3e^\alpha - 1 = (e^\alpha - 1)^3 > 0$ since $\alpha > 0$.

Consider now the numerator. The numerator evaluated at $\alpha = 0$ is 0. We want to show that it is positive for all other α , and therefore the numerator is positive for all $\alpha > 0$. Let $e^\alpha = \mu$ and let's factor out the positive term $e^{-\alpha \gamma}$. We are left to examine:

$$\mu^{2+\gamma} + \mu^{1+\gamma} - (\gamma + 1)^2 \mu^2 + (2\gamma^2 + 2\gamma - 1) \mu - \gamma^2.$$

Differentiating with respect to μ :

$$\frac{d\kappa}{d\mu} = (2 + \gamma) \mu^{1+\gamma} + (1 + \gamma) \mu^\gamma - 2(\gamma + 1)^2 \mu + (2\gamma^2 + 2\gamma - 1).$$

Evaluating at $\mu = 1$:

$$\left. \frac{d\kappa}{d\mu} \right|_{\mu=1} = (2 + \gamma) + 1 + \gamma - 2(\gamma + 1)^2 + (2\gamma^2 + 2\gamma - 1) = 0.$$

Differentiating again:

$$\frac{d^2 \kappa}{d\mu^2} = (1 + \gamma)(2 + \gamma) \mu^\gamma + (1 + \gamma) \gamma \mu^{\gamma-1} - 2(\gamma + 1)^2,$$

$$\left. \frac{d^2 \kappa}{d\mu^2} \right|_{\mu=1} = (1 + \gamma)(2 + \gamma) + (1 + \gamma) \gamma - 2(\gamma + 1)^2 = 0,$$

$$\frac{d^3 \kappa}{d\mu^3} = (1 + \gamma)(2 + \gamma) \gamma \mu^{\gamma-1} + (1 + \gamma) \gamma \mu^{\gamma-2}.$$

Since all quantities in the above equation are positive, the third derivative κ of is positive for all $\mu \geq 1$. Note also, κ that and its first and second derivatives are 0 at $\mu = 1$, which implies that the first and second derivatives of κ as well as κ itself must be positive for all $\mu > 1$. This in turn implies that $\frac{d^2 h}{d\alpha^2}$ is positive for all $\alpha > 0$ and the function g is convex for all $\lambda > 0$.

To prove the monotonic descent property, we note that $h(\alpha)$ is monotonically decreasing if and only if $g(\lambda)$ is monotonically decreasing:

$$\begin{aligned} \frac{dh}{d\alpha} &= - \frac{e^{-\alpha \gamma} (e^{\alpha \gamma + \alpha} + (1 - e^\alpha) \gamma - e^\alpha)}{(e^\alpha - 1)^2} \\ &= - \frac{e^{-\alpha \gamma} (e^\alpha (e^{\alpha \gamma} - 1) + (1 - e^\alpha) \gamma)}{(e^\alpha - 1)^2} < 0. \end{aligned}$$

For all $\alpha > 0$. Consequently $g(\lambda)$ is monotonically decreasing. \square

Theorem 2. Stochastic ordering of susceptible and infectious populations.

Let A_i^S be the random variable distributed as f_i^S , and similarly A_i^I as $f_i^I(\lambda)$.

Then, as long as $f_0^S(\lambda), f_0^I(\lambda)$ are non-deterministic, for any $i > 0$:

$$A_{i+1}^S <_{ST} A_i^S \quad \text{for } \lambda \geq E_i^S(\lambda), \quad (\text{A.9})$$

$$A_i^S <_{ST} A_{i+1}^I \quad \text{for } \lambda \geq E_i^S(\lambda), \quad (\text{A.10})$$

$$A_{i+1}^I <_{ST} A_i^I \quad \text{for } \lambda \geq E_i^I(\lambda), \quad (\text{A.11})$$

where $X <_{ST} Y$ implies that X is strictly smaller than Y in the usual stochastic order.

Proof. Take any $i > 0$:

$$\begin{aligned} f_{i+1}^S(\lambda) &= \frac{(1 - p_i(I|\lambda)) f_i^S(\lambda)}{\sum_0^\infty (1 - p_i(I|\lambda)) f_i^S(\lambda)} = f_i^S(\lambda) \frac{(e^{-\lambda p \beta_i})}{\sum_0^\infty (e^{-\lambda p \beta_i}) f_i^S(\lambda)} \\ &= f_i^S(\lambda) \frac{(e^{-\lambda p \beta_i})}{E_i^S(e^{-\lambda p \beta_i})} \end{aligned}$$

Since $\beta_i > 0$, $e^{-\lambda p \beta_i}$ is strictly monotonically decreasing in λ . Therefore:

$$\frac{f_{i+1}^S(\lambda)}{f_i^S(\lambda)} = \frac{(e^{-\lambda p \beta_i})}{E_i^S(e^{-\lambda p \beta_i})}$$

is strictly monotonically decreasing in λ implying that A_{i+1}^S is smaller than A_i^S in likelihood ratio order, which in turn implies Eq. (9). See Shaked and Shanthikumar for further detail [24]:

$$f_{i+1}^l(\lambda) = \frac{p_i(l|\lambda) \text{astf}_i^S(\lambda)}{\sum_0^\infty p_i(l|\lambda) f_i^S(\lambda)} = f_i^S(\lambda) \frac{(1 - e^{-\lambda p \beta_i})}{E_i^S(1 - e^{-\lambda p \beta_i})}.$$

Here $(1 - e^{-\lambda p \beta_i})$ is strictly monotonically increasing, so:

$$\frac{f_i^S(\lambda)}{f_{i+1}^l(\lambda)} = \frac{E_i^S(1 - e^{-\lambda p \beta_i})}{(1 - e^{-\lambda p \beta_i})}.$$

Is strictly monotonically decreasing in λ , implying Eq. (10).

Finally,

$$f_i^l(\lambda) = C_i^l \left(e^{-\lambda p \sum_{j=0}^{i-2} \beta_j} - e^{-\lambda p \sum_{j=0}^{i-1} \beta_j} \right) f_0^S(\lambda) = \frac{C_i^l}{C_i^S} (e^{\lambda p \beta_{i-1}} - 1) f_i^S(\lambda),$$

$$f_i^S(\lambda) = \frac{\frac{C_i^S}{C_i^l} f_i^l(\lambda)}{(e^{\lambda p \beta_{i-1}} - 1)},$$

Furthermore:

$$\begin{aligned} f_{i+1}^l(\lambda) &= f_i^S(\lambda) \frac{(1 - e^{-\lambda p \beta_i})}{E_i^S(1 - e^{-\lambda p \beta_i})} = \frac{\frac{C_i^S}{C_i^l} f_i^l(\lambda)}{(e^{\lambda p \beta_{i-1}} - 1)} * \frac{(1 - e^{-\lambda p \beta_i})}{\frac{C_i^S}{C_i^l} E_i^l \left(\frac{(1 - e^{-\lambda p \beta_i})}{(e^{\lambda p \beta_{i-1}} - 1)} \right)} \\ &= f_i^l(\lambda) \frac{\left(\frac{(1 - e^{-\lambda p \beta_i})}{(e^{\lambda p \beta_{i-1}} - 1)} \right)}{E_i^l \left(\frac{(1 - e^{-\lambda p \beta_i})}{(e^{\lambda p \beta_{i-1}} - 1)} \right)}. \end{aligned}$$

From the definition of β_i , and the fact that $i > 0$; $\beta_{i-1} > 0$ and $\beta_i > 0$.

From Lemma 1, we know that $\left(\frac{(1 - e^{-\lambda p \beta_i})}{(e^{\lambda p \beta_{i-1}} - 1)} \right)$ is monotonically decreasing, so:

$$\frac{f_{i+1}^l(\lambda)}{f_i^l(\lambda)} = \frac{\left(\frac{(1 - e^{-\lambda p \beta_i})}{(e^{\lambda p \beta_{i-1}} - 1)} \right)}{E_i^l \left(\frac{(1 - e^{-\lambda p \beta_i})}{(e^{\lambda p \beta_{i-1}} - 1)} \right)}$$

is monotonically decreasing, and Eq. (11) is proved. \square

Theorem 3. As long as $f_0^S(\lambda), f_0^l(\lambda)$ are non-deterministic, for any $i > 0$:

$$f_i^S(\lambda) > f_{i+1}^S(\lambda) \quad \text{for } \lambda \geq E_i^S(\lambda), \quad (\text{A.12})$$

$$f_i^S(\lambda) < f_{i+1}^l(\lambda) \quad \text{for } \lambda \geq E_i^S(\lambda), \quad (\text{A.13})$$

$$f_i^l(\lambda) > f_{i+1}^l(\lambda) \quad \text{for } \lambda \geq E_i^l(\lambda), \quad (\text{A.14})$$

regardless of initial contact rate distribution.

Proof. Take any $i > 0$.

By Jensen's inequality, since $e^{-\lambda p \beta_i}$ is a strictly convex function, $e^{-E_i^S(\lambda) p \beta_i} < E_i^S(e^{-\lambda p \beta_i})$

Furthermore, since $e^{-\lambda p \beta_i}$ is strictly decreasing, whenever $\lambda \geq E_i^S(\lambda)$.

$e^{-\lambda p \beta_i} \leq e^{-E_i^S(\lambda) p \beta_i} < E_i^S(e^{-\lambda p \beta_i})$, and using the derivation from Theorem 2.

$$f_{i+1}^S(\lambda) = f_i^S(\lambda) \frac{(e^{-\lambda p \beta_i})}{E_i^S(e^{-\lambda p \beta_i})} < f_i^S(\lambda), \text{ proving Eq. (12).}$$

Now for Eq. (13), note that since $f_0^S(\lambda)$ is non-deterministic and $\lambda \geq 0, E_i^S(\lambda) > 0$. We are interested in $\lambda \geq E_i^S(\lambda) > 0$.

Since $(1 - e^{-\lambda p \beta_i})$ is strictly concave for $\lambda > 0$, we again use Jensen's inequality, to show that:

$$1 - e^{-E_i^S(\lambda) p \beta_i} > E_i^S(1 - e^{-\lambda p \beta_i})$$

$$\text{whenever } \lambda \geq E_i^S(\lambda) 1 - e^{-\lambda p \beta_i} \geq 1 - e^{-E_i^S(\lambda) p \beta_i} > E_i^S(1 - e^{-\lambda p \beta_i});$$

$$f_{i+1}^l(\lambda) = f_i^S(\lambda) \frac{(1 - e^{-\lambda p \beta_i})}{E_i^S(1 - e^{-\lambda p \beta_i})} > f_i^S(\lambda).$$

Finally, we use Jensen's inequality for the third time for the last equation. Recall from Lemma 1, $\left(\frac{(1 - e^{-\lambda p \beta_i})}{(e^{\lambda p \beta_{i-1}} - 1)} \right)$ that is monotonically decreasing and convex for $\lambda > 0$.

Whenever $\lambda \geq E_i^l(\lambda)$:

$$\left(\frac{(1 - e^{-\lambda p \beta_i})}{(e^{\lambda p \beta_{i-1}} - 1)} \right) \leq \left(\frac{(1 - e^{-E_i^l(\lambda) p \beta_i})}{(e^{E_i^l(\lambda) p \beta_{i-1}} - 1)} \right) < E_i^l \left(\frac{(1 - e^{-\lambda p \beta_i})}{(e^{\lambda p \beta_{i-1}} - 1)} \right),$$

and

$$f_{i+1}^l(\lambda) < f_i^l(\lambda). \quad \square$$

Corollary 1. For $i > 0$, and $f_0^S(\lambda), f_0^l(\lambda)$ non deterministic:

$$E_i^S(\lambda) < E_{i+1}^S(\lambda), \quad (\text{A.15})$$

$$E_i^l(\lambda) < E_{i+1}^l(\lambda). \quad (\text{A.16})$$

Proof. The proof follows immediately from the stochastic ordering of A_i^S and A_i^l . \square

Appendix B. Supplementary material

Supplementary data associated with this article can be found, in the online version, at doi:10.1016/j.ejor.2012.01.027.

References

- [1] R.M. Anderson, R.M. May, Infectious Diseases of Humans: Dynamics and Control, Oxford University Press, Oxford, UK, 1991.
- [2] H. Andersson, T. Britton, Stochastic Epidemic Models and Their Statistical Analysis, Springer-Verlag, New York, 2000 (Chapter 6).
- [3] Centers for Disease Control and Prevention: 2009 H1N1 Early Outbreak and Disease Characteristics. Available at: <<http://www.cdc.gov/h1n1flu/surveillanceqa.htm>> (accessed 25.02.11).
- [4] Centers for Disease Control and Prevention: Questions and Answers: Seasonal Flu Shot. Available at: <<http://www.cdc.gov/FLU/about/qa/flushot.htm>> (accessed 20.01.11).
- [5] Centers for Disease Control and Prevention: Updated CDC Estimates of 2009 H1N1 Influenza Cases, Hospitalizations and Deaths in the United States, April 2009 – March 13, 2010. Available at: <http://www.cdc.gov/h1n1flu/estimates/April_March_13.htm> (accessed 25.02.11).
- [6] Central Intelligence Agency: The World Factbook. Available at: <<https://www.cia.gov/library/publications/the-world-factbook/index.html>> (accessed 25.02.11).
- [7] O. Diekmann, J.A.P. Heesterbeek, Mathematical Epidemiology of Infectious Diseases: Model Building, Analysis and Interpretation, Wiley, 2000.
- [8] O. Diekmann, J.A.P. Heesterbeek, J.A.J. Metz, On the definition and the computation of the basic reproduction ratio R_0 in models for infectious diseases in heterogeneous populations, Journal of Mathematical Biology 28 (4) (1990) 354–382.
- [9] R.G. Gallager, Discrete Stochastic Processes, Kluwer Academic Publishers, Boston, MA, 1996.
- [10] H.W. Hethcote, J.W. Van Ark, Epidemiological models for heterogeneous populations: Proportionate mixing, parameter estimation, and immunization programs, Mathematical Bioscience 84 (1) (1987) 85–118.
- [11] W.O. Kermack, A.G. McKendrick, A contribution to the mathematical theory of epidemics, Proceedings of the Royal Society of London Series A 115 (1927) 700–721.
- [12] R.C. Larson, Simple models of influenza progression within a heterogeneous population, Operations Research 55 (3) (2007) 399–412.
- [13] J.O. Lloyd-Smith et al., Superspreading and the effect of individual variation on disease emergence, Nature 438 (2005) 355–359.
- [14] I. Longini, E. Halloran, Strategy for distribution of influenza vaccine to high-risk groups and children, American Journal of Epidemiology 161 (4) (2005) 303–306.
- [15] M. Lupis, SARS Patient Zeros: Chinese Doctor's Research Causes Epidemic. <http://www.masternewmedia.org/2003/04/12/sars_patient_zero_chinese_doctors.htm>, 2003 (accessed 25.02.11).

- [19] R.M. May, Network structure and the biology of populations, *Trends in Ecology & Evolution* 21 (2006) 394–399.
- [20] J. Mossong et al., Social contacts and mixing patterns relevant to the spread of infectious diseases, *PLoS Medicine* (2008).
- [21] K.R. Nigmatulina, Modeling and Responding to Pandemic Influenza: Importance of Population Distributional Attributes and Non-Pharmaceutical Interventions. Doctoral Dissertation. Retrieved from: <<http://dspace.mit.edu/handle/1721.1/53298>>, 2009 (accessed 25.02.11).
- [22] K.R. Nigmatulina, R.C. Larson, Living with influenza: Impacts of government imposed and voluntarily selected interventions, *European Journal of Operations Research* 195 (2) (2009) 613–627.
- [23] A. Nold, Heterogeneity in disease transmission modeling, *Mathematical Biosciences* 52 (1980) 227–240.
- [24] M. Shaked, G.J. Shanthikumar, *Stochastic Orders*, Springer Science, New York, 2007 (Chapter 1).
- [25] K. Shi, J. Lu, H. Fan, et al., Rationality of 17 cities' public perception of SARS and predictive model of psychological behavior, *Chinese Science Bulletin* 48 (13) (2003) 1297–1303.
- [26] M. Small, C.K. Tse, D.M. Walker, Super-spreaders and the rate of transmission of the SARS virus, *Physica D: Nonlinear Phenomena* 240 (8) (2006) 695–804.
- [27] J.K. Taubenberger, D.M. Morens, 1918 Influenza: The mother of all pandemics, *Emerg Infect Dis* [serial on the Internet]. 2006 Jan. doi:10.3201/eid1209.05-0979.
- [28] A.R. Tuite et al., Estimated epidemiologic parameters and morbidity associated with pandemic H1N1 influenza, *Canadian Medical Association Journal* 182 (2) (2010) 131–136.
- [29] Typhoid Mary Dies of a Stroke At 68. Carrier of Disease, Blamed for 51 Cases and 3 Deaths, but She Was Held Immune. *The New York Times*, 1938 (accessed 25.02.11).
- [30] P. van den Driessche, J. Watmough, Reproduction numbers and sub-threshold endemic equilibria for compartmental models of disease transmission, *Mathematical Biosciences* 180 (2002) 29–48.
- [31] L.F. White et al., Estimation of the reproductive number and the serial interval in early phase of the 2009 influenza A/H1N1 pandemic in the USA, *Influenza and Other Respiratory Viruses* 3 (2009) 267–276, doi:10.1111/j.1750-2659.2009.00106.x.

Further reading

- [3] E. Bender, E. Canfield, The asymptotic number of labelled graphs with given degree sequences, *Journal of Combinatorial Theory A* 24 (1978) 296–307.
- [4] T. Britton, M. Deijfen, M.L. Anders, Generating simple random graphs with prescribed degree distribution, *Journal of Statistical Physics* 124 (6) (2006) 1377–1397.
- [11] P. Erdős, A. Rényi, On random graphs, *Publicationes Mathematicae* 6 (1959) 290–297.